ELSEVIER

Journal of Alloys and Compounds 323–324 (2001) 763–767

Journal of ALLOYS AND COMPOUNDS

www.elsevier.com/locate/jallcom

Stark level structure and oscillator strengths of Nd^{3+} ion in different fluoride single crystals

I.R. Martín[a,*], Y. Guyot[b], M.F. Joubert[b], R.Yu. Abdulsabirov[c], S.L. Korableva[c], V.V. Semashko[c]

[a]*Departamento de Física Fundamental y Experimental, Universidad de La Laguna, 38206 La Laguna, Tenerife, Spain*

[b]*Laboratoire de Physico–Chimie des Matériaux Luminescents. UMR CNRS N° 5620, Université de Lyon 1, 43 boulevard 11 Novembre 1918, 6922 Villeurbanne Cedex, France*

[c]*Laboratory of Quantum Electronics and Radiospectroscopy, Kazan State University, 18 Kremlin Street, 420008 Kazan, Russia*

Abstract

Optical properties of three fluoride single crystals (YF_3, $LiLuF_4$ and KY_3F_{10}) doped with Nd^{3+} ions have been studied. Low temperature absorption spectra lead to the Stark energy level scheme up to 29 000 cm^{-1}. From room temperature absorption measurements and using the Judd–Ofelt theory, the Ω_2, Ω_4 and Ω_6 parameters have been obtained in the $LiLuF_4$:Nd^{3+} and KY_3F_{10}:Nd^{3+} crystals and radiative lifetimes have been calculated.

Keywords: Light absorption and reflection; Luminescence; Optical properties

1. Introduction

Recently there has been considerable progress in the development of up-conversion lasers based on rare earth doped materials [1]. It has been shown for the Nd^{3+} ions that the operation of up-conversion laser in the blue to ultraviolet (UV) spectral regions depends strongly on the crystal host [2,3]. It is therefore important to understand the factors determining the lifetimes of the $^2P_{3/2}$ and $^4D_{3/2}$ upper states of the $4f^n$ configuration of Nd^{3+} incorporated in different surroundings. These emitting levels of the Nd^{3+} ions have rather small energy gaps to the levels below them and the low phonon frequencies of the fluorides result in good quantum efficiencies for blue or near UV luminescence from these levels. $^4F_{3/2}$ is also an important energy level to investigate as it can serve as population reservoir for different scheme of up-conversion pumping and because it is a well known starting level for infrared (IR) stimulated emissions.

In this work the optical properties of the Nd^{3+} ions have been studied in three fluoride single crystals (YF_3, $LiLuF_4$ and KY_3F_{10}). Raman spectra have been done to estimate the highest vibrational frequency in each host. Judd–Ofelt parameters were derived from the absorption spectra and used to calculate the radiative lifetimes of the $^4F_{3/2}$, $^4D_{3/2}$ and $^2P_{3/2}$ levels in the different crystals. Moreover, the absorption spectra obtained at liquid helium temperature permit to obtain the energy level schemes for the Stark components of the Nd^{3+} manifolds in these crystals.

2. Experimental

The samples studied (YF_3:Nd^{3+}, $LiLuF_4$:Nd^{3+} and KY_3F_{10}:Nd^{3+}) were grown from carbon crucibles using the Stockbarger method. As determined by electron beam micro-probe analysis, the Nd^{3+} concentration is 4.13 10^{19} at cm^{-3} (0.29 at.%) in Nd:$LiLuF_4$ (refractive index 1.468, thickness 0.304 cm with the crystallographic c axis perpendicular to this thickness) and 2.37 10^{20} at cm^{-3} (1.51 at.%) in Nd:KY_3F_{10} (refractive index 1.4712 and thickness 0.359 cm). The Nd:YF_3 crystal is too small for the concentration to be measured but 1% of Nd was introduced during the growth; it is also too small to be oriented and cut along the crystallographic directions, so we did not record polarized spectra with it.

Absorption spectra in the range from 200 to 900 nm were recorded using a Cary 2300 Varian Spectrophotometer equipped with a continuous flow helium refrigerator. Experimental fluorescence decays were measured under pulsed laser excitation at 355 nm (for the $^4D_{3/2}$ and $^2P_{3/2}$ decays) or at 733 nm (for the $^4F_{3/2}$ decays). Raman spectra

*Corresponding author.

0925-8388/01/$ – see front matter
PII: S0925-8388(01)01080-5

were performed using an Ar^+ laser and a Dilor XY triple spectrometer.

3. Results and discussion

The absorption spectra of the YF_3:Nd^{3+}, $LiLuF_4$:Nd^{3+} and KY_3F_{10}:Nd^{3+} crystals have been measured in the 200–900 nm range at liquid helium temperature and at room temperature. As example, Fig. 1 presents the room temperature absorption spectrum obtained with the KY_3F_{10}:Nd^{3+} crystal. The transitions observed correspond to $4f^3 \rightarrow 4f^3$ electronic transitions of Nd^{3+} ions and they are clearly identified by comparison with the results obtained in other crystals [4,5].

From the spectra obtained with high resolution at liquid helium temperature, it has been possible to determine the position of the Stark components of the Nd^{3+} manifolds from $^4F_{3/2}$ to the near UV (see Table 1).

From the absorption spectra obtained at room temperature in the $LiLuF_4$:Nd^{3+} (σ and π polarized spectra) and KY_3F_{10}:Nd^{3+} crystals the oscillator strengths were calculated using the expression

$$f = \frac{mc^2}{\pi e^2 N} \frac{2.303}{d} \int \frac{\mathrm{OD}(\lambda)\, \mathrm{d}\lambda}{\lambda^2} \quad (1)$$

where m and e are the electron mass and charge respectively, c is the velocity of the light, OD(λ) the optical density as a function of wavelength and d is the sample thickness. The oscillator strength values for the $LiLuF_4$:Nd^{3+} crystal have been calculated as a contribution of the values obtained in the σ and π polarized spectra ($f = 2f_\sigma/3 + f_\pi/3$). The values obtained for the

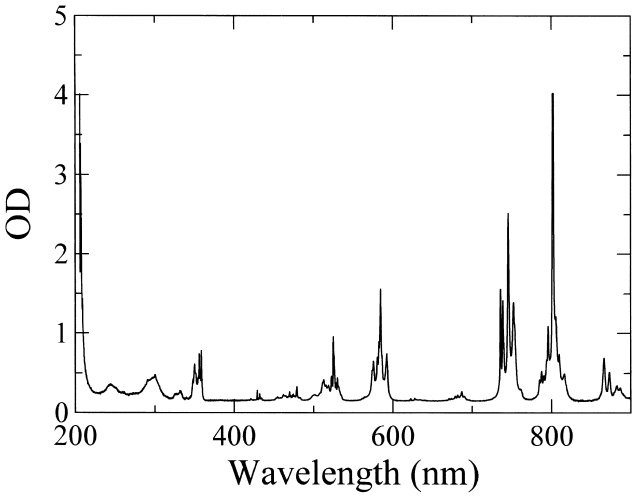

Fig. 1. Absorption spectrum obtained at room temperature in a KY_3F_{10} crystal doped with Nd^{3+}.

Table 1
Experimental energy levels for Nd^{3+} in YF_3, $LiLuF_4$ and KY_3F_{10} crystals

Transition	E (cm^{-1})		
	YF_3	KY_3F_{10}	$LiLuF_4$
$^4F_{3/2}$	11 532	11 441	11 603
	11 674	11 543	
$^4F_{5/2} + {}^2H(2)_{9/2}$	12 561	12 458	12 538
	12 566	12 465	12 545
	12 601	12 468	12 629
	12 671	12 571	12 635
	12 686	12 595	12 669
	12 696	12 650	12 731
	12 754	12 693	12 817
	12 859	12 742	
$^4F_{7/2}$,$^4S_{3/2}$	13 477	13 409	13 497
	13 587	13 513	13 522
	13 654	12 531	13 645
	13 697	13 583	13 651
	13 710	13 596	13 662
	13 740		
$^4F_{9/2}$	14 790	14 669	14 750
	14 833	14 735	14 779
	14 901	14 766	14 880
	14 921	14 847	14 893
	15 005	14 914	14 954
$^2H(2)_{11/2}$	16 019	15 888	15 866
	16 044	15 928	15 967
	16 059	16 028	16 055
	16 088	16 060	16 144
	16 107		
	16 123		
$^4G_{5/2}$	17 271	17 125	17 154
	17 336	17 169	17 266
	17 414	17 222	17 289
$^2G(1)_{7/2}$	17 455	17 339	17 407
	17 489	17 357	17 417[a]
	17 524	17 370	17 472
	17 564	17 398	17 651
$^4G_{7/2}$	19 133	18 997	19 056
	19 223	19 042	19 069
	19 242	19 108	19 175
	19 316	19 138	19 199
$^4G_{9/2} + {}^2K_{13/2}$	19 618	19 432	19 652
	19 668	19 550	19 708
	19 693	19 579	19 751[a]
	19 730	19 606	
	19 755	19 677	
	20 100		
$^2K_{15/2}$, $^2G(1)_{9/2}$, $^2D(1)_{3/2}$,$^4G_{11/2}$	21 010[a]	20 987	21 015
	21 114	21 019	21 043
	21 211	21 072	21 054
	21 315	21 114[a]	21 063
	21 397	21 215	21 213[a]
	21 547[a]	21 292	21 270[a]
	21 570	21 360	21 315

Table 1. Continued

Transition	E (cm^{-1})		
	YF_3	KY_3F_{10}	$LiLuF_4$
$^2K_{15/2}$, $^2G(1)_{9/2}$, $^2D(1)_{3/2}$, $^4G_{11/2}$	21 603	21 486	21 420
	21 645[a]	21 596	21 434
	21 727	21 639	21 538[a]
	22 087	21 713	21 545[a]
	22 101	21 858	21 985
		22 008[a]	22 394[a]
$^2P_{1/2}$	23 427	23 308	23 386[a]
$^2D(1)_{5/2}$	23 745	23 716	23 738
	23 840	23 744	23 886
	24 009	23 898	24 041
		23 949[b]	
$^2P_{3/2}$		26 109	
$^4D_{3/2}$	28 202	27 995	28 093
	28 257	28 096	28 197
$^4D_{5/2}$	28 438	28 403	28 345
	28 547	28 471	28 527
	28 641	28 545	
$^4D_{1/2}$	28 922	28 722	28 781

[a] Less accurate results (very weak lines).
[b] This line is less intense than the three others in this $^2D(1)_{5/2}$ range.

$LiLuF_4$:Nd^{3+} and KY_3F_{10}:Nd^{3+} crystals are presented in Tables 2 and 3.

The experimental oscillator strength values have been used to calculate the Ω_λ values corresponding to the Judd–Ofelt theory [6,7]. Using this theory the calculated oscillator strengths can be obtained as

Table 3
Measured and calculated oscillator strengths obtained at room temperature in a KY_3F_{10} crystal doped with Nd^{3+} ions, all transitions are from the $^4I_{9/2}$ level

Transition	λ(nm)	f_m (*10^{-8})	f_c (*10^{-8})
$^4F_{3/2}$	870	207.3	223.5
$^4F_{5/2}$, $^2H(2)_{9/2}$	802	922.4	869.8
$^4F_{7/2}$, $^4S_{3/2}$	746	897.3	985.9
$^4F_{9/2}$	687	74.0	73.4
$^2H(2)_{11/2}$	627.5	18.9	20.4
$^4G_{5/2}$, $^2G(1)_{7/2}$	585.0	1033.9	1049.1
$^2K_{13/2}$, $^4G_{7/2}$, $^4G_{9/2}$	525	730.4	530.6
$^2K_{15/2}$, $^2G(1)_{9/2}$, $^2D(1)_{3/2}$, $^4G_{11/2}$	470	239.2	139.2
$^2P_{1/2}$	429	37.0	50.6
$^2D(1)_{5/2}$	421	2.4	5.6
$^2P_{3/2}$	383	7.3	4.4
$^4D_{3/2}$, $^4D_{5/2}$, $^4D_{1/2}$, $^2I_{11/2}$, $^2L_{15/2}$	355	1040.6	1093.7
$^2I_{13/2}$, $^4D_{7/2}$, $^2L_{17/2}$	329	203.1	*
$^2H(1)_{9/2}$, $^2D(2)_{3/2}$, $^2H(1)_{11/2}$, $^2D(2)_{5/2}$	300	1747.0	*
$^2F(2)_{5/2}$, $^2F(2)_{7/2}$	244	799.3	*

[*] These UV peaks are not included in the calculation in order to get nice fits.

$$f(aJ;bJ') = \frac{8\pi^2 m\nu}{3h(2J+1)e^2 n^2}\left[X_{\mathrm{DE}}S_{\mathrm{DE}}(aJ;bJ') + X_{\mathrm{DM}}S_{\mathrm{DM}}(aJ;bJ')\right] \quad (2)$$

where $X_{\mathrm{ED}} = n(n^2+2)^2/9$, $X_{\mathrm{MD}} = n^3$, n is the refractive index and the strength lines, $S_{\mathrm{ED}}(aJ;bJ')$ and $S_{\mathrm{MD}}(aJ;bJ')$ are given by

$$S_{\mathrm{DE}}(aJ;bJ') = e^2\sum_\lambda \Omega_\lambda |\langle f^n\gamma[SL]JM_J\|U^{(\lambda)}\|f^n\gamma'[S'L']J'M'_J\rangle|^2 \quad (3)$$

Table 2
Measured and calculated oscillator strengths obtained at room temperature in a $LiLuF_4$ crystal doped with Nd^{3+} ions, all transitions are from the $^4I_{9/2}$ level

Transition	λ(nm)	f_m (*10^{-8})	f_c(*10^{-8})
$^4F_{3/2}$	862.5	90.3	84.3
$^4F_{5/2}$, $^2H(2)_{9/2}$	791.5	475.8	429.2
$^4F_{7/2}$, $^4S_{3/2}$	740	465.1	522.2
$^4F_{9/2}$	677	29.9	38.0
$^2H(2)_{11/2}$	627	14.5	10.3
$^4G_{5/2}$, $^2G(1)_{7/2}$	585.5	521.9	529.4
$^2K_{13/2}$, $^4G_{7/2}$, $^4G_{9/2}$	521.5	333.4	236.6
$^2K_{15/2}$, $^2G(1)_{9/2}$, $^2D(1)_{3/2}$, $^4G_{11/2}$	478	102.1	60.7
$^2P_{1/2}$	431	12.0	15.3
$^2D(1)_{5/2}$	no experimental transition	–	–
$^2P_{3/2}$	no experimental transition	–	–
$^4D_{3/2}$, $^4D_{5/2}$, $^4D_{1/2}$, $^2I_{11/2}$, $^2L_{15/2}$	350	348.9	380.0
$^2I_{13/2}$, $^4D_{7/2}$, $^2L_{17/2}$	330	66.5	*
$^2H(1)_{9/2}$, $^2D(2)_{3/2}$, $^2H(1)_{11/2}$, $^2D(2)_{5/2}$	295	185.8	*
$^2F(2)_{5/2}$, $^2F(2)_{7/2}$	260	9.7	*

[*] These UV peaks are not included in the calculation in order to get nice fits.

Table 4
Judd–Ofelt parameters ($\times 10^{-20}$ cm^2) obtained in different crystals

Crystal	Ω_2	Ω_4	Ω_6	Ω_4/Ω_6
$LiLuF_4$	1.19	1.27	4.04	0.31
KY_3F_{10}	1.37	4.16	7.56	0.55
$LiYF_4$ [9]	1.22	2.10	4.65	0.45
$LiKYF_5$ [10]	0.92	3.21	4.26	0.75
$YAl_3(BO_3)_4$ [11]	3.09	5.04	3.11	1.62

$$S_{MD}(aJ;bJ') = \left[\frac{e\hbar}{2mc}\right]^2 |f^n\gamma[SL]JM_J\|\vec{L} + 2\vec{S}\|f^n\gamma'[S'L']J'M_J'\rangle|^2 \quad (4)$$

It is known that the reduced matrix elements of the unit tensor $U^{(\lambda)}$ are almost insensitive to the ion environment. We have used the $U^{(\lambda)}$ parameters given in Ref. [8]. The Judd–Ofelt parameters Ω_λ found at least-square fitting of the experimental oscillator strength values given by Eq. (2) to the experimental ones are given in Table 4. These values are compared to those ones found in other matrices [9–11].

The well known IR laser transition, corresponding to the $^4F_{3/2} \rightarrow {}^4I_{11/2}$ transition, depends only on the Ω_4 and Ω_6 parameters due to the reduced matrix elements of the unit tensor $U^{(\lambda=2)}$ which are equal to zero. Therefore, for a large cross-section for this transition, Ω_4 and Ω_6 are required to be as large as possible. Moreover, Ω_2 does not enter the branching ratios for the $^4F_{3/2}$ fluorescence, so these ones can be expressed in terms of the Ω_4/Ω_6 ratio [8]. In order to maximize the fluorescence intensity to $^4I_{11/2}$ relatively to emission to $^4I_{9/2}$, $^4I_{13/2}$ and $^4I_{15/2}$, one requires $\Omega_4 << \Omega_6$. Comparing the values presented in the Table 4, it is expected that

1. the KY_3F_{10}:Nd^{3+} crystal presents the highest value for the $^4F_{3/2} \rightarrow {}^4I_{11/2}$ stimulated emission cross section,
2. the $LiLuF_4$:Nd^{3+} crystal presents the most favorable branching ratio for the $^4F_{3/2} \rightarrow {}^4I_{11/2}$ transition.

The Ω_λ parameters found with the absorption measurements have been also used to calculate the spontaneous emission probabilities from the $^4F_{3/2}$ to the ^4I_J (J=15/2, 13/2, 11/2, 9/2) and from the $^4D_{3/2}$ and the $^2P_{3/2}$ manifolds to all the lower levels. In the Judd–Ofelt theory [6,7], the spontaneous emission probabilities between two levels are given by

Table 6
Measured and calculated lifetimes (μs) and highest phonon values (cm^{-1}) obtained in different crystals

Crystal	τ_m	τ_c	$E_{phonon\ max}$
$LiLuF_4$:0.29at%Nd	495	722	500
KY_3F_{10}:1.51at%Nd	260	334	602
YF_3	240	–	550
$LiYF_4$:0.1at%Nd [9]	550	538	500
$LiKYF_5$:0.3at%Nd [10]	475	558	440
$YAl_3(BO_3)_4$:5.6at%Nd [11]	53	302	1300

$$A(aJ;bJ') = \frac{64\pi^4\nu^3}{3h(2J+1)c^3}[X_{DE}S_{DE}(aJ;bJ') + X_{DM}S_{DM}(aJ;bJ')] \quad (5)$$

and the radiative lifetime of and excited level aJ is given by

$$\tau = \sum_{bJ'} \frac{1}{A(aJ;bJ')} \quad (6)$$

where the sum is extended over all the states at energies lower than aJ. The branching ratios for the different emissions with the same initial level are

$$\beta(A(aJ;bJ')) = \frac{A(aJ;bJ')}{\sum_{bJ'} A(aJ;bJ')} \quad (7)$$

In Table 5 are presented the calculated values for the spontaneous emission probabilities and branching ratios from the $^4F_{3/2}$ level in the $LiLuF_4$:Nd^{3+} and KY_3F_{10}:Nd^{3+} crystals. As it is expected, attending to the values of the ratio Ω_4/Ω_6 presented in Table 4, the $LiLuF_4$ crystal presents the highest value for the branching ratio of the $^4F_{3/2} \rightarrow {}^4I_{11/2}$ transition.

The calculated values for the spontaneous emission probabilities lead to the τ_c lifetimes given in Table 6. In this table are also indicated the measured fluorescence decay time constants τ_m as well as the highest phonon values measured in the Raman spectra. The large energy gap between $^4F_{3/2}$ and the next lower level suggests that the fact that the measured decay rate is shorter than the calculated radiative lifetime is due to energy transfers between Nd^{3+} ions. Indeed, to measure radiative lifetime of $^4F_{3/2}$, it would be necessary to have extremely low concentrated crystals thus avoiding interactions between

Table 5
Calculated spontaneous emission probabilities A (s^{-1}) and branching ratios β for the $^4F_{3/2}$ level in different crystals

Transition	$LiLuF_4$		KY_3F_{10}		$LiYF_4$ [9]	$LiKYF_5$ [10]	$YAl_3(BO_3)_4$ [11]
					β	β	β
	A	β	A	β			
$^4I_{9/2}$	407.4	0.29	1066	0.36	0.33	0.392	0.49
$^4I_{11/2}$	787.0	0.57	1570	0.52	0.54	0.5	0.43
$^4I_{13/2}$	181.3	0.13	341.2	0.11	0.12	0.103	0.07
$^4I_{15/2}$	9.3	0.01	17.6	0.01	0.01	0.005	0.01

active ions. Concerning the $^4D_{3/2}$ and the $^2P_{3/2}$ manifolds, their calculated radiative lifetimes are respectively 85 μs and 675 μs in $LiLuF_4:Nd^{3+}$, and 32 μs and 314 μs in $KY_3F_{10}:Nd^{3+}$. Experimentally, we measured 1 ± 0.1 μs and 19 ± 1.9 μs for $^4D_{3/2}$ and $^2P_{3/2}$ respectively in our two crystals ($LiLuF_4$: 0.29 at.% Nd and KY_3F_{10}: 1.51 at.% Nd). These measured fluorescence decay times reflect energy transfers between Nd^{3+} ions as well as probably single-ion non-radiative relaxations.

4. Conclusions

This work is first an investigation of the Stark level structure of Nd^{3+} ions in the three fluoride crystals $YF_3:Nd^{3+}$, $LiLuF_4:Nd^{3+}$ and $KY_3F_{10}:Nd^{3+}$; it is complementary to preliminary results related essentially to the ^4I term and the $^4F_{3/2}$ manifold [8]. Raman spectra and Judd–Ofelt analysis of room temperature absorption spectra reveal interesting properties for the $LiLuF_4$ host: low phonon cutoff and high branching ratio for the $^4F_{3/2}\rightarrow{}^4I_{11/2}$ transition.

Acknowledgements

This work was partially supported by the INTAS program (contract number INTAS-97-787), 'Gobierno Autónomo de Canarias (PI1999/100)' and 'Comisión Interministerial de Ciencia y Tecnología (PB98-0437)'.

References

[1] R. Scheps, Prog. Quant. Electr. 20 (1996) 271.
[2] R.M. Macfarlane, F. Tong, A.J. Silversmith, W. Lenth, Appl. Phys. Lett. 16 (1988) 1300.
[3] W. Lenth, R.M. Macfarlane, J. Lumin. 45 (1990) 346.
[4] A.A.S. da Gamma, F. Gilberto De Sá, P. Porcher, P. Caro, J. Chem. Phys. 75 (1981) 2385.
[5] M.F. Joubert, B. Jacquier, C. Linares, R.M. Macfarlane, J. Lumin. 47 (1991) 269.
[6] B.R. Judd, Phys. Rev. 127 (1962) 750.
[7] G.S. Ofelt, J. Chem. Phys. 37 (1962) 511.
[8] A.A. Kaminskii, in: M.J. Weber (Ed.), Crystalline Lasers: Physical Processes and Operating Schemes, CRC Press, 1996.
[9] C. Li, Y. Guyot, C. Linarè s, R. Moncorgé, M.F. Joubert, in: A.A. Pinto, T.Y. Fan (Eds.), Osa Proceedings On Advanced Solid State Lasers, Vol. 15, 1993, pp. 91–95, New Orleans.
[10] A.A. Kaminskii et al., Phys. Stat. Solidi (a) 145 (1994) 177.
[11] D. Jaque, J. Capmany, Z.D. Luo, J. García Solé, J. Phys.: Cond. Matter 9 (1997) 9715, D Jaque. Ph.D. Thesis. Universidad Autónoma de Madrid. 1999.